

Analysis of molecular mechanism for acceleration of polyembryony using gene functional annotation pipeline in *Copidosoma floridanum*

Takuma Sakamoto

Tokyo Noko Daigaku Nogakubu Daigakuin Nogaku Kenkyuin

Maaya Nishiko

Tokyo Noko Daigaku Nogakubu Daigakuin Nogaku Kenkyuin

Hidemasa Bono

Joho System Kenkyu Kiko Life Science Togo Database Center

Takeru Nakazato

Joho System Kenkyu Kiko Life Science Togo Database Center

Jin Yoshimura

Shizuoka Daigaku

Hiroko Tabunoki (✉ h_tabuno@cc.tuat.ac.jp)

Tokyo Noko Daigaku <https://orcid.org/0000-0003-1823-9952>

Kikuo Iwabuchi

Tokyo Noko Daigaku Nogakubu Daigakuin Nogaku Kenkyuin

Research article

Keywords: Polyembryony, XDH, Endoparasitoid, Polyembryogenesis, *Copidosoma floridanum*

Posted Date: May 14th, 2019

DOI: <https://doi.org/10.21203/rs.2.9609/v1>

License: © ⓘ This work is licensed under a Creative Commons Attribution 4.0 International License.

[Read Full License](#)

Version of Record: A version of this preprint was published on February 11th, 2020. See the published version at <https://doi.org/10.1186/s12864-020-6559-3>.

Abstract

Background: Polyembryony, when several embryos are clonally produced from a single egg, is found in humans, armadillo, and some endoparasitoid insects. Thus, although polyembryony is conserved through insects to mammals, the polyembryogenesis progress remains obscure in these animals. The polyembryonic parasitoid wasp *Copidosoma floridanum* oviposits its egg into the host insect egg, and, eventually, >2000 individuals occur from one egg. We reported previously that polyembryogenesis was enhanced by juvenile hormone (JH) treatment under the culture condition. Hence, we performed RNA-Seq analysis to elucidate the molecular mechanisms in controlling polyembryogenesis using *C. floridanum*. Nevertheless, *C. floridanum* genes do not have a functional gene annotation because of partial whole-genome sequence elucidation. Hence, we constructed a gene functional annotation pipeline for *C. floridanum* and performed a molecular network analysis in *C. floridanum*. Results: We extracted fluctuated genes from control and JH treatment molura after 48-h culture to assess molecular mechanisms in polyembryogenesis. Consequently, we obtained 11,117 transcripts and 217 differentially expressed genes in the JH treatment group compared with the control group. Whereas, we used the blastp program to assign whole *C. floridanum* transcripts to human gene. Remarkably, 76% of *C. floridanum* transcripts were assigned to human genes. Moreover, we determined platelet degranulation and fatty acid biosynthetic process, suppressing cell morphogenesis involved in the differentiation and integrin signaling pathway by the gene enrichment analysis in the JH treatment group compared with the control group. Furthermore, we noted that molecular interaction possibly associated with polyembryogenesis using Cytoscape. Conclusions: In this study, we constructed *C. floridanum* gene functional annotation pipeline and *C. floridanum* transcripts shared with homology to human genes during early embryo developmental stage. Additionally, this study establishes new molecular interactions associated with polyembryogenesis; these molecules could elucidate molecular mechanism in polyembryony, suggesting a possibility of using the molecular interaction in twinning of humans.

Background

Typically, higher-order animals develop from one egg to one individual by cell cleavage; however, some animals always develop through polyembryogenesis which many embryos are produced from one embryo from one egg. Although identical twin is representative examples of human polyembryogenesis, their likelihood is as low as 0.3% [1]. Reportedly, armadillos (the genus *Dasypus*) are the only mammals that exhibit obligatory polyembryony by developing from one egg to four individuals after embryonic shield separation [2,3]. As experiments using mammals have ethical limitations, the phenomenon of polyembryogenesis remains partially elucidated. Moreover, cultured cell lines, such as mouse and human cancer cell line, and tissue culture method have not been established in armadillos.

Remarkably, new polyembryogenesis cases have been reported for insects, such as endoparasitic wasps Braconidae, Dryinidae, Platygasteridae, and Encyrtidae, and research on developmental patterns has witnessed progress lately [4]. Thus, although polyembryony is conserved through insects to mammals, the polyembryogenesis process remains obscure in these animals. Elucidation of polyembryogenesis-

related molecular mechanisms could markedly further our understanding of the mechanisms for regulating polyembryogenesis in animals.

Endoparasitic wasp, *Copidosoma floridanum* (Hymenoptera: Encyrtidae) is an egg-larval parasitoid of the pluriine moth *Thysanoplusia intermixta*. *T. intermixta* egg developmental stage is four days, a larval developmental stage is around twenty days, and a pupal developmental stage is around eight days under experimental condition [5] (Fig.1). In the usual experimental condition, *C. floridanum* parasitizes until 2-day old egg in *T. intermixta*. *C. floridanum* produces nearly 2000 cloned embryos from one fertilized egg developing into a female or an unfertilized egg developing into a male (Fig.1). Although almost all insects exhibit egg segmentation by the superficial cleavage, *C. floridanum* egg segments by the holoblastic cleavage. The *C. floridanum* egg starts cleavage when laid into the host egg (Fig. 1a). Then, the *C. floridanum* egg starts developing from the two-cell stage to morula after *C. floridanum* embryo invades into their host embryo (Fig. 1b). The egg of *C. floridanum* is composed of an embryonic cell and an anterior cell from a polar body [6]. The anterior cell develops to an extraembryonic syncytium which constitutes the outer side of the morula. The extraembryonic syncytium from the anterior cell starts wrapping around the blastomeres after chorion was removed from eggshell and then will be morula (Fig. 1c). As early morulae have motility, they can invade the host embryo, and then morulae will be developed to polyembryos when morulae movement are stopped into host embryo [7] (Fig. 1d). Then, a part of polyembryos starts to develop to soldier larvae through soldier embryo (Fig. 1e and f). Each embryo attains morphogenesis when the host insect develops to the end of the final instar larvae (Fig. 1g). Finally, reproductive larvae emerge when the host insect achieve on the second day of final instar larvae (Fig. 1h), and adults emerge from the mummy (Fig. 1i) [8,9]. Thus, although it was known how *C. floridanum* polyembryony is progressed into the host embryo, its molecular mechanisms remain obscure.

Previously, we reported that the development of polyembryo is accelerated by juvenile hormone (JH) treatment or JH analog methoprene under the culture condition [10]. Although the molecular function of JH remains unclear in embryogenesis of *C. floridanum*, we anticipated that JH or methoprene act as an initiator to promote polyembryogenesis from two-cell to polymorula stage. Nevertheless, *C. floridanum* genes do not have a functional gene annotation because of partial whole-genome sequence elucidation. Thus, we cannot analyze molecular networks in *C. floridanum* like *Drosophila melanogaster*, a model insect. Accordingly, we constructed a gene functional annotation pipeline for *C. floridanum* and conducted a molecular network analysis in *C. floridanum*, focusing on the gene expression when polyembryony is promoted by JH treatment in the embryo of the two-cell developmental stage. We also performed RNA-Seq analysis using *C. floridanum* as a model animal of polyembryogenesis for elucidation molecular mechanisms.

Results

Juvenile hormone accelerates polyembryogenesis

We collected the two-cell stage embryos and cultured for 5 days; then, we counted the cultured embryo and assessed whether these embryos were polymoluræ or not (Fig. 2). Consequently, the JH treatment group exhibited an increased rate of polymoluræ compared with the control group. Additionally, the JH treatment group displayed polymoluræ from 2 days after culture, whereas the control group displayed polymoluræ from 4 days after culture. Hence, the developmental span for presenting polymoluræ was shortened in the JH treatment group compared with the control group (Fig. 2; Table 1).

Extraction of differentially expressed genes and assignment of human homolog

First, we constructed the *C. floridanum* functional gene annotation pipeline (Fig. 3). Upon adding JH to the culture medium, polymoluræ appeared after 2 days. Hence, we obtained the total RNA for the RNA-Seq analysis after 48-h cell culture. Then, we performed the RNA-Seq analysis in three control samples (SRA accession numbers: DRR138914, DRR138915, and DRR138916) and two JH-treated samples (DRR138917 and DRR138918). These RNA-Seq data were mapped with HISAT2 and StringTie, and we obtained 11,117 transcripts from these RNA-Seq data. Then, we searched for transcripts that were commonly expressed between the control and JH treatment groups; we found 10,908 transcripts.

Comparison of the gene expression between the JH treatment group and the control group by the TCC package using read-count data yielded 217 differentially expressed transcripts [DEGs; false discovery rate (FDR) <0.05; Fig. 4a]. While the expression of 123 transcripts was increased, that of 94 transcripts was decreased in the JH treatment group (Fig. 4a, orange-colored dots indicate fluctuated transcripts in the JH treatment group).

Then, we assessed the number of *C. floridanum* genes by comparing our transcripts dataset and the *C. floridanum* RefSeq datasets. Of 11,117 transcripts in the *C. floridanum* RNA-Seq datasets, we identified 9417 transcripts in the *C. floridanum* RefSeq datasets (covered 84.7%). Furthermore, we assessed the number of human homologs in the *C. floridanum* transcripts. We identified 6098 human homologs of 11,117 total transcripts in the *C. floridanum* using the tblastx program with a cutoff *E* value at $1e^{-10}$. Of 217 *C. floridanum* genes whose expression alters when comparing the JH treatment and control groups, 88 genes corresponded to human genes.

Gene enrichment analysis of DEG

To examine Gene enrichment analysis, we chose 88 genes between the JH treatment group and the control group, the expression of 42 genes was elevated in the JH treatment group, whereas the expression of 46 genes was down-regulated in the JH treatment group. We imported the list of DEGs for these genes, and their expression levels into Metascape. Metascape were converted to human homologs for the gene enrichment analysis. Metascape generated 12 genetic function groups as Gene Ontology (GO) presenting a significant correlation for the GO of platelet degranulation (GO:0002576), and fatty acid biosynthetic

process (GO:0006633) was upregulated in the JH treatment group (Fig. 4b). Furthermore, Metascape suggested 12 genetic function groups as GO, whose expression of cell morphogenesis was involved in differentiation (GO: 0000904) and ST Integrin Signaling Pathway (M3270); the gene expression constituting these GOs was downregulated in the JH treatment group (Fig. 4c).

Screening for related molecules using the molecular network analysis by Cytoscape

We focused on the GO terms platelet degranulation, fatty acid biosynthetic process, and integrin signaling pathway to identify the molecular network that correlates with polyembryogenesis. Using the public protein interaction database and Cytoscape, we further explored correlations among the genes involved in platelet degranulation, fatty acid biosynthetic process, and integrin signaling pathway. Hence, we identified the molecular interaction including filamin-A (*FLNA*), xanthine dehydrogenase/oxidase (*XDH*), exportin-1 (*XPO1*), protein phosphatase slingshot homolog 2 (*SSH2*), and integrin alpha-4 (*ITGA4*) as fluctuated genes in the JH treatment group (Fig. 5a); these molecules associated with this pathway were plotted on the graph using Transcripts Per Kilobase Million (TPM) value (Fig. 5b). We found that the *FLNA* and *XDH* mRNA expression was increased, while that of *SSH2* and *ITGA4* was decreased in the JH treatment group (Fig. 5b). However, the *XPO1* mRNA expression was not altered between the control and JH treatment groups (Fig. 5b).

Discussion

This study investigated the gene expression when polyembryogenesis is promoted by JH treatment of the embryo in the two-cell developmental stage of *C. floridanum*. Additionally, we constructed the functional gene annotation pipeline for *C. floridanum* and performed a molecular network analysis in *C. floridanum*.

Previously, we reported that polyembryogenesis is accelerated by JH treatment and methoprene under the cell culture condition [10]; this phenomenon was also established when JH I and JH II were added to the culture medium [10]. Of all compounds, methoprene promoted polyembryogenesis the most. However, farnesol, farnesyl acetate, or methyl caproate did not promote polyembryogenesis [10]. Moreover, polyembryogenesis was not promoted upon adding ecdysone to the culture medium (Supplementary Fig. 1). Hence, only JH or methoprene promotes polyembryogenesis in *C. floridanum*.

JH is a unique hormone that is present in insects; it has -, -unsaturated methyl ester groups and epoxy groups, which are crucial for JH function, at both ends of a molecule having a terpenoid backbone [11]. Reportedly, JH plays several vital roles such as regulation of molting, pheromone biosynthesis, maturation of gonads, development of eggs, maintaining homeostasis, maintenance of population, and body color change [12]. Hence, JH is extensively involved in insect physiology.

We assessed the expression of Krüppel homolog 1 (*Kr-h1*), which is one of the JH responsive genes, to validate whether molura responds to JH or not [13]. However, the *Kr-h1* mRNA expression was not altered

between the control and JH treatment groups (Supplementary Fig. 2). Retinoid X receptor (RXR), a type of nuclear receptor that binds to 9-cis retinoic acid [14], could bind to several types of chemicals that share the chemical structure of retinoic acid [15]. Reportedly, JH analog of methoprene and methoprene acid can bind to RXR [15]. Besides, RXR can bind to JH as a JH receptor in *D. melanogaster* [16]. Hence, in this study, we focused on *C. floridanum* RXR-alpha-B (LOC106637147) and validated the mRNA expression; the expression of *C. floridanum* RXR-alpha-B was increased in the JH treatment group (Supplementary Fig. 2). Retinoic acid associates with embryonic development and cell differentiation through RXR [17], suggesting that JH could act such as retinoic acid for embryonic development. Accordingly, JH could act like the retinoic acid signaling pathway in our polyembryony model.

Subsequently, we performed the gene expression analysis by RNA-Seq to explicate the molecular mechanism of polyembryogenesis in morula by JH treatment. Nevertheless, our RNA-Seq analysis had to be performed during the early proliferative phases in the polyembryony of *C. floridanum*. Hence, we collected samples for purification of the total RNA one day before polyembryogenesis by JH treatment. Using the gene functional annotation pipeline that we have developed, we identified 6098 human homologs of 11,117 total transcripts in *C. floridanum* and determined that 55% of *C. floridanum* polyembryo transcripts were homologous to human genes. Assumedly, our transcriptome data might not include larval morphogenesis and body colored genes (data not shown).

Additionally, *C. floridanum* RefSeq datasets were constructed by analyzing male and female adult *C. floridanum* transcriptome. A study reported analyzing a reference genome sequence of *C. floridanum* using male adult (https://www.ncbi.nlm.nih.gov/assembly/GCF_000648655.2/). Overall, 17,038 of estimated proteins were registered in the NCBI Genome database (https://www.ncbi.nlm.nih.gov/genome/12734?genome_assembly_id=358239). Furthermore, we identified 13,160 human homologs of 17,308 total predicted protein dataset in *C. floridanum* using the current gene functional annotation pipeline. Surprisingly, *C. floridanum* has 76% of human homologous genes.

Previously, we identified human homologs in *Bombyx mori* and *D. melanogaster* by systematic BLAST search. *B. mori* and *D. melanogaster* contained 8469 and 8815 human homologs, respectively [18]. Therefore, a large number of human homologs are conserved in *C. floridanum* genes compared with these model insects. In this study, 88 *C. floridanum* genes corresponded to human genes whose expression fluctuates when comparing JH treatment and control, and we input these genes to gene enrichment and molecular network analyses.

The gene enrichment analysis revealed that the expression of lipid metabolism-related (GO: 0006633) and platelet degranulation (GO: 0002576) genes were increased in the JH treatment group. An analysis of the characteristics of these genes containing GO terms revealed the involvement of vesicle-associated V-soluble N-ethylmaleimide-sensitive factor attachment protein receptor (SNARE) in cellular membrane adhesion [19]. Additionally, synaptosomal-associated protein (*SNAP*)25 and 29, (*SNAPC*) 3 and 4, SNARE-associated protein Snapin (*SNAPIN*), and syntaxin-binding protein (*STXBP*) were identified as gene whose

expressions were common in the JH treatment and control groups; reportedly, these are involved in the membrane fusion in neurosecretory cells [20]. Notably, syntaxin-binding protein (*STXBP*) complexes these proteins and inactivates the cellular membrane fusion [20]. In *C. floridanum*, the *STXBP* mRNA expression was downregulated in the JH treatment group. Perhaps, cellular membrane fusion could be activated by *STXBP* downregulation in the JH treatment group. As the morula promotes fusion with the extraembryonic syncytium by the JH treatment, morula could be accelerated to polyembrogenesis.

Remarkably, *SNAP25* and *SNAP29*, *SNAPC3* and *SNAPC4*, *SNAPIN* and *STXBP* were expressed in *C. floridanum* morula embryos; these genes also play a role in neurosecretory cells of humans [21]. Hence, *C. floridanum* might use similar molecular mechanisms of cellular membrane adhesion as human neurosecretory cells. Furthermore, we found that the expression of integrin pathway-related genes involved in focal adhesion (M3270: ST Integrin Signaling Pathway) was downregulated in the JH treatment.

The morula comprises the outer extraembryonic syncytium and the inner embryonic cell; the extraembryonic syncytium separates by dividing the embryonic cell [22]. Of note, embryonic cells adhere to the extraembryonic syncytium through integrin in the morula. When the integrin expression is decreased by the JH treatment, perhaps, the connection is loose in embryonic cells and the extraembryonic syncytium. Consequently, the extraembryonic syncytium invaginates into the cell gap of embryonic cells and these might divide, enabling us to find new molecular relationships by Cytoscape. *FLNA*, an actin filament crosslinking protein in non-muscle cells [23], might be involved in the division of embryos interacting with *SSH2* and *ITGA4*. Reportedly, *SSH2* mediates actin dynamics [24], and *ITGA4* belongs to the integrin family and plays a role in cell adhesion [25].

XDH is a rate-limiting enzyme involved in purine metabolism and key enzyme for uric acid synthesis. In the *B. mori* egg development, the amount of uric acid gradually declines until the blastokinesis stage but then increases until the egg pigmentation stage [26]. Remarkably, knocking down of XDH enhanced the cell mobility and invasion in HepG2 cells; however, XDH did not affect cell proliferation [27]. XDH converts retinoic acid to 9-cis retinal [28]. Moreover, the XDH activity is essential for JH action to bristle formation and cuticle production on the abdominal epidermis during pupal and adult development [29].

The chemical structure of JH III and retinoic acid is similar and, perhaps, JH III binds to XDH. XDH-bound JH could enter the nucleus via *XPO1*, and released JH might bind to RXR to control subsequent transcription; this molecular correlation could be a novel association triggered by JH. Accordingly, the following model could be considered in the process of forming morula to polymolura. The embryos are wrapped with the extraembryonic syncytium (Fig. 6a). In the formation of polymolurae, actin degradation was avoided by reducing the *SSH2* expression, followed by suppressing the *ITGA4* expression. As the connection between embryonic cells and embryonic cells is loose (Fig. 6b), the syncytial membrane facilitates fractionation (Fig. 6c and d) in embryonic cells and promotes polyembryony (Fig. 6e). Hence, XDH plays a key role in embryogenesis via JH, besides uric acid synthesis. Overall, this study determines

novel molecular interactions associated with polyembryogenesis and demonstrates a connection of these molecules needed to progress polyembryogenesis for cell separation.

Conclusions

In this study, we construct *C. floridanum* gene functional annotation pipeline and *C. floridanum* transcripts sharing homology to several human genes during the early embryo development stage. Remarkably, *C. floridanum* has many human homologs compared with *D. melanogaster*. Additionally, we present new molecular interactions associated with polyembryogenesis, which would elucidate molecular mechanism in polyembryony, suggesting a possibility of using the molecular interaction in polyembryogenesis of humans. In future studies, we intend to investigate the function of these molecules using RNAi in *C. floridanum*.

Methods

Insect

We obtained *C. floridanum* from parasitized *T. intermixta* larvae from burdock fields in Tokyo, Chiba, and Ibaraki Prefectures. Larvae were maintained with an artificial diet [30] at 25°C with a 16-h light/8-h dark cycle. *T. intermixta* adults were fed a 10% sugar solution absorbed with cotton. *C. floridanum* adults were fed a 50% honey solution absorbed with cotton. We used *T. intermixta* eggs within 17 h post-oviposition for parasitism by *C. floridanum*. The parasitized hosts were kept in the same conditions as non-parasitized hosts.

Embryo culture

We dissected the two-cell stage of the embryo from *T. intermixta* eggs within 2-h post-oviposition and, then, cultured it with the modified MGM medium [31]. We dissolved JH III (J2000; Sigma-Aldrich Co. Ltd., Munich, Germany) in ethanol to prepare a stock solution (10 mg/mL); then, 1 L of this stock solution was added to the modified MGM medium as the final concentration was 1 g/mL.

RNA-Seq analysis

We isolated the total RNA from 2-day cultured morulae using a combination of TRIzol LS Reagent and PureLink RNA Extraction Kit (Thermo Fisher Scientific Inc., Valencia, CA) per the manufacturer's instructions. Then, we used an Agilent TapeStation 2200 (Agilent Technologies, Santa Clara, CA) to assess the RNA quality. Additionally, single-end sequencing cDNA libraries were constructed with 100 ng of total RNA from these samples (control group: $n = 3$; JH group: $n = 2$) with a TruSeq Stranded mRNA Sample Preparation Kit (Illumina Inc., San Diego, CA) per the manufacturer's instructions. Next, libraries

were sequenced (75 bp, single-end) on the Illumina NextSeq500 platform, and FASTQ files were assessed by Trim Galore! v0.4.5 (https://www.bioinformatics.babraham.ac.uk/projects/trim_galore/). Notably, the *C. floridanum* genome (GCF_000648655.2) sequence is available in the NCBI Genome database (https://www.ncbi.nlm.nih.gov/genome/annotation_euk/Copidosoma_floridanum/101/). The obtained FASTQ sequence files were aligned to the genomic reference sequence by HISAT2 v2.1.0 with default parameters [32]. Next, SAM files were converted to BAM files by Samtools v1.8 [33]. Using StringTie v1.3.4, we estimated the transcript abundance, and the count data were extracted by Subread v1.6.0 [34,35]. All statistical analyses were performed using R software version 3.4.3 (<https://www.r-project.org>), the TCC package, and the DEseq2 package [36]. We generated a scatter plot using TIBCO Spotfire Desktop v7.6.0 with the “Better World” program license (TIBCO Spot re, Inc., Palo Alto, CA; <http://spotfire.tibco.com/better-world-donation-program/>). Furthermore, the sequence data (FASTQ files) were deposited to the DDBJ Sequence Read Archive (accession numbers DRR138914-DRR138918).

***C. floridanum* gene functional annotation pipeline for molecular network analysis**

We mapped *C. floridanum* transcripts to *C. floridanum*'s genome sequence using the gffread program (<https://github.com/gperte/gffread>). To annotate *C. floridanum* gene, we identified genes homologous to those of human by conducting a systematic BLAST search (tblastx) with a cutoff E-value of significant homology at $1e-10$ (query: *C. floridanum* cDNA sequence; database: whole human cDNA sequence set from Ensembl database). Using the generated assignment table, we reconstructed conserved pathways common to *C. floridanum* and humans by projecting *C. floridanum* genes onto the human pathway.

Gene enrichment analysis and pathway analysis

We performed the gene enrichment analysis using Metascape (<http://metascape.org/>); a gene list for Metascape analysis was generated from the TCC output. Then, we performed the molecular network analysis using IntAct Molecular Interaction Database (<https://www.ebi.ac.uk/intact/>) and Cytoscape v3.6.1 (<http://www.cytoscape.org>). We converted the gene IDs from the *C. floridanum* RNA-Seq data to human Ensembl IDs, using the assignment table described above and, then, input the list of genes obtained from the RNA-Seq data into Cytoscape to obtain the significant molecular interactions with corresponding *E* values.

List Of Abbreviations

DEG Differentially expressed genes

GO Gene Ontology

JH Juvenile hormone

RQ Relative quantification

RXR Retinoid X receptor

SNARE Sensitive factor attachment protein receptor

TPM Transcripts Per Kilobase Million

Declarations

Ethics approval and consent to participate

Not applicable.

Consent to publish

Not applicable.

Availability of data and materials

The RNA-seq reads supporting the conclusions of this article are available in the Sequence Read Archive (SRA) with accession IDs: DRR138914, DRR138915, and DRR138916 ; control samples, DRR138917 and DRR138918 ;JH-treated samples.

Competing interests

The authors declare that they have no competing interests.

Funding

This work was supported by JSPS KAKENHI grant number JP15H02483 to Kil, JY and HT, 15H04420 to JY, 26257405 to JY, 18H02212 to HT.

The funders declare that they have no role for the design of the study and collection, analysis, and interpretation of data and in writing the manuscript.

Authors' contributions

Conceived and designed the experiments: T.S, H.T, and Ki.I.. Performed the experiments: T.S and M.N. Contributed reagents/materials/analysis tools: J.Y., Ki.I, and H.T. Analyzed the data: T.S, H.B, T.N. and H.T.

Contributed to the writing of the paper under draft version: T.S. and H.T. All authors discussed the data and helped with manuscript preparation. Ki.I. and H.T. supervised the project. All authors read and approved the final manuscript.

Acknowledgement

We thank to Dr. Madoka Nakai, Tokyo University of Agriculture and Technology for helpful discussion.

References

1. Tong S, Caddy D, Short R V. Use of dizygotic to monozygotic twinning ratio as a measure of fertility. *Lancet*. 1997;349(9055):843–845.
2. Enders AC. Implantation in the nine-banded armadillo: How does a single blastocyst form four embryos? *Placenta*. 2002;23(1):71–85.
3. Loughry W. J., Prodöhl, P. A., McDonough, C. M., Avise, J. C. Polyembryony in armadillos. *American Scientist*. 1998;86:274-279.
4. Ivanova-Kasas OM (1972) Polyembryony in insects. In: Counce SJ, Waddington CH (eds) *Developmental systems*, vol 1. Academic Press, New York, pp 243–271
5. Uematsu H. The effective temperature and seasonal prevalence of *Thysanoplusia intermixta* (WARREN) (Lepidoptera: Noctuidae) *Proc. Assoc. Pl. Prot. Kyushu* 1978; 24:109-112
6. Baehrecke EH., Strand MR., Embryonic morphology and growth of the polyembryonic parasitoid *Copidosoma floridanum* (Ashmead) (Hymenoptera : Encyrtidae) *International J. Insect Morphol. and Embryology* 1990; 19(3–4):165-175
7. Nakaguchi A, Hiraoka T, Endo Y, Iwabuchi K. Compatible invasion of a phylogenetically distant host embryo by a hymenopteran parasitoid embryo. *Cell Tissue Res*. 2006; 324(1):167–173.
8. Strand MR. Oviposition behavior and progeny allocation of the polyembryonic wasp *Copidosoma floridanum* (Hymenoptera: Encyrtidae). *J Insect Behav*. 1989; 2(3):355–369.
9. Grbic M, Nagy LM, Carroll SB, Strand M. Polyembryonic development: insect pattern formation in a cellularized environment. *Development*. 1996; 122(3):795–804.
10. Iwabuchi K. Effect of juvenile hormone on the embryogenesis of a polyembryonic wasp, *Copidosoma floridanum*, in vitro. *Vitr Cell Dev Biol - Anim J Soc Vitro Biol*. 1995; 31(10):803–805.
11. Gilbert LI, A. Granger N, Roe RM. The juvenile hormones: Historical facts and speculations on future research directions. *Insect Biochem Mol Biol*. 2000; 30(8–9):617–644.

12. Truman JW, Riddiford LM. The origins of insect metamorphosis. *Nature*. 1999; 401(6752):447–452.
13. Adam G. The retinoic-like juvenile hormone controls the looping of left-right asymmetric organs in *Drosophila*. *Development*. 2003; 130(11):2397–2406.
14. Germain P, Germain P, Chambon P, Eichele G, Evans RM, Lazar MA, et al. International Union of Pharmacology . LXIII . Retinoid X Receptors. *Pharmacological Reviews* 2006; 58(4):760-772
15. Harmon MA, Boehm MF, Heyman RA, Mangelsdorf DJ. Activation of mammalian retinoid X receptors by the insect growth regulator methoprene. *Proc Natl Acad Sci*. 1995; 92(13):6157–6160.
16. Jones G, Jones D. Considerations on the structural evidence of a ligand-binding function of ultraspiracle, an insect homolog of vertebrate RXR. *Insect Biochem Mol Biol*. 2000; 30(8–9):671–679.
17. Grenier E, Levy E, Tremblay E, Delvin E, Garofalo C, Sane A, et al. Effect of retinoic acid on cell proliferation and differentiation as well as on lipid synthesis, lipoprotein secretion, and apolipoprotein biogenesis. *Am J Physiol Liver Physiol*. 2007; 293(6):G1178– G1189.
18. Tabunoki H, Bono H, Ito K, Yokoyama T. Can the silkworm (*Bombyx mori*) be used as a human disease model? *Drug Discov Ther*. 2016; 10(1):3–8.
19. Chen X, Tomchick DR, Kovrigin E, Araç D, Machius M, Sü TC. Three-Dimensional Structure of the Complexin/SNARE Complex energy of SNARE complex formation may be used to overcome the energy barrier required to bring the synaptic vesicle and plasma membranes together, perhaps. *Neuron* 2002; 33:397–409.
20. Mohrmann R, De Wit H, Verhage M, Neher E, Sørensen JB. Fast vesicle fusion in living cells requires at least three SNARE complexes. *Science*. 2010; 330(6003):502–505.
21. Südhof TC. Neurotransmitter release: The last millisecond in the life of a synaptic vesicle. *Neuron*. 2013; 80(3):675–690.
22. Grbić M, Nagy LM, Strand MR. Development of polyembryonic insects: A major departure from typical insect embryogenesis. *Dev Genes Evol*. 1998; 208(2):69–81.
23. Nakamura F, Stossel TP, Hartwig JH. The filamins: organizers of cell structure and function. *Cell Adh Migr*. 2011; 5(2):160–169.
24. Niwa R, Nagata-Ohashi K, Takeichi M, Mizuno K, Uemura T. Control of actin reorganization by slingshot, a family of phosphatases that dephosphorylate ADF/cofilin. *Cell*. 2002; 108(2):233–246.
25. Yang JT, Rayburn H, Hynes RO., Cell adhesion events mediated by alpha 4 integrins are essential in placental and cardiac development. *Development*. 1995; 121(2):549-560.

26. Hayashi Y, Studies on the xanthine oxidase system in the silkworm, *Bombyx mori* L. (III) Changes of the uric acid content and xanthine dehydrogenase activity in the silkworm egg during embryonic development. *Bull. Sericul. Exp. Stat.* 1961; 30(6):427-436
27. Chen GL, Ye T, Chen HL, Zhao ZY, Tang WQ, Wang LS, et al. Xanthine dehydrogenase downregulation promotes TGF β signaling and cancer stem cell-related gene expression in hepatocellular carcinoma. *Oncogenesis.* 2017; 6(9):e382.
28. Taibi G, Di Gaudio F, Nicotra CMA. Xanthine dehydrogenase processes retinol to retinoic acid in human mammary epithelial cells. *J Enzyme Inhib Med Chem.* 2008; 23(3):317–327.
29. Zhou X, Riddiford LM: rosy function is required for juvenile hormone effects in *Drosophila melanogaster*. *Genetics.* 2008, 178: 273-281.
30. Kawasaki K, Ikeuchi M, Hidaka T. Laboratory rearing method for *Acanthopplusia agnata* (Lepidoptera: Noctuidae) without change of artificial diet. *Japanese J Appl Entomol Zool.* 1987; 31(1):78–80.
31. Iwabuchi K. Early Embryonic Development of a Polyembryonic Wasp, *Litomastix maculata* Ishii, in vivo and in vitro. *Appl Entomol Zool.* 1991; 26(4):563–570.
32. Pertea M, Kim D, Pertea GM, Leek JT, Salzberg SL. Transcript-level expression analysis of RNA-seq experiments with HISAT, StringTie and Ballgown. *Nat Protoc.* 2016; 11:1650.
33. Wysoker A, Fennell T, Marth G, Abecasis G, Ruan J, Li H, et al. The Sequence Alignment/Map format and SAMtools. *Bioinformatics.* 2009; 25(16):2078–2079.
34. Liao Y, Smyth GK, Shi W. The Subread aligner: Fast, accurate and scalable read mapping by seed-and-vote. *Nucleic Acids Res.* 2013; 41(10):e108.
35. Liao Y, Smyth GK, Shi W. featureCounts: an efficient general purpose program for assigning sequence reads to genomic features. *Bioinformatics.* 2014; 30(7):923–930.
36. Sun J, Nishiyama T, Shimizu K, Kadota K. TCC: An R package for comparing tag count data with robust normalization strategies. *BMC Bioinformatics.* 2013;14:219

Table

Table 1. Impact of polyembryogenesis by the juvenile hormone treatment to the early embryo of *Copidosoma floridanum*

Treatment groups	Day of polymorula	Rate of polymorula (%)
1	4.88 ± 0.13	25.0
2	3.16 ± 0.23	60.3

Treatment group 1 ($n = 57$) was treated without JH; treatment group 2 ($n = 57$) was treated with JH.

Figures

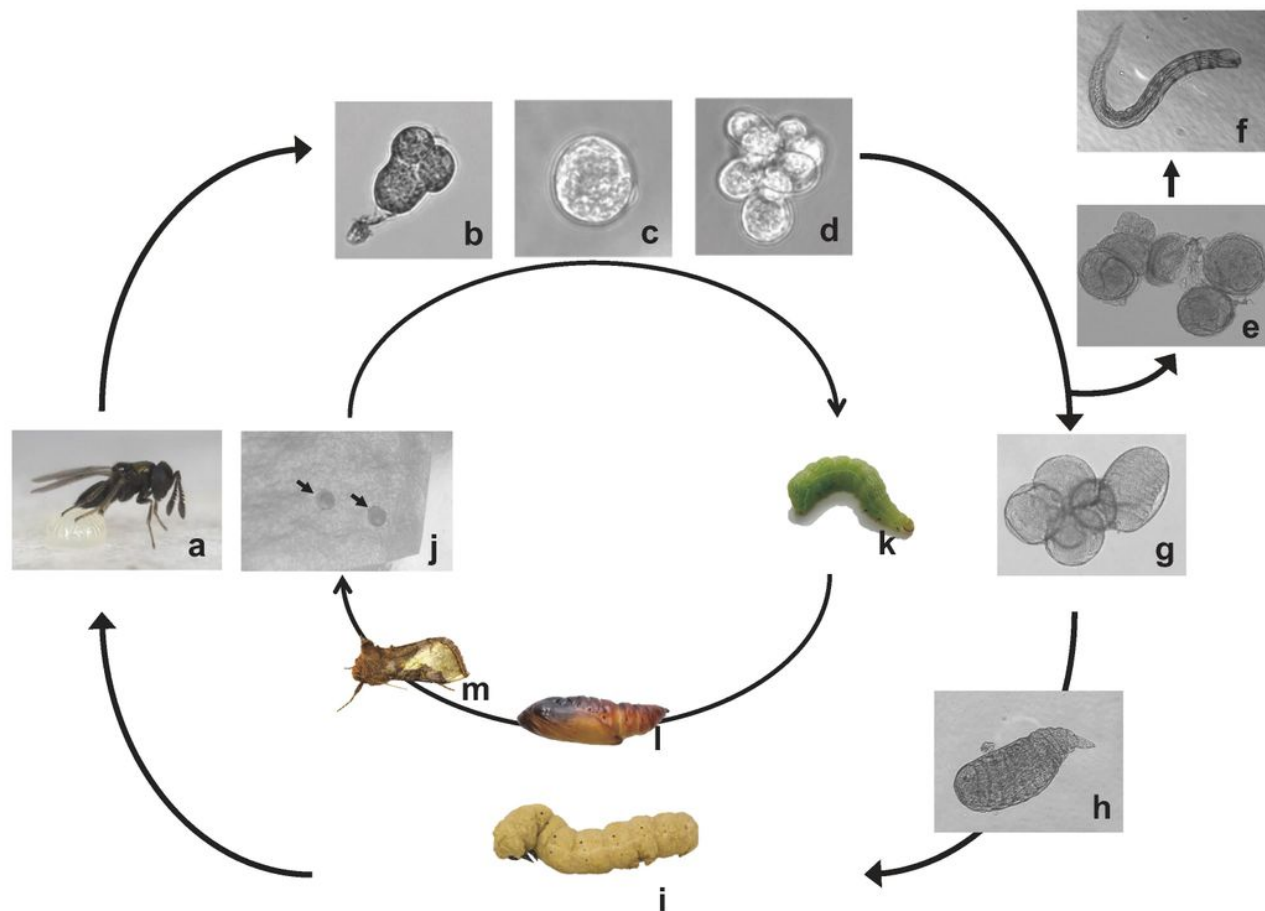


Figure 1

The life cycle of *Copidosoma floridanum*. *C. floridanum* oviposited its egg into the host egg (a). Then, the *C. floridanum* egg starts developing from the two-cell stage to morula and invaginates into host the embryo (b and c). The morula embryo is clonally divided, and polyembryos are formed around 60 h after

parasitism after invading the host embryo (d). A part of polyembryos starts segmentation and, then, develops into soldier larvae via soldier embryo (e and f). Each embryo achieves morphogenesis when the host insect develops at the end of the fifth instar larvae (g) and, then, reproductive larva appears (h). Finally, reproductive larvae emerge when the host insect achieves on the second day of sixth instar larvae, and the adult emerges from the mummy (i). j-m: *T. intermixta* life cycle. (j) *T. intermixta* egg indicates black arrows. (k) final (sixth) instar larva. (l) pupa, (m) adult.

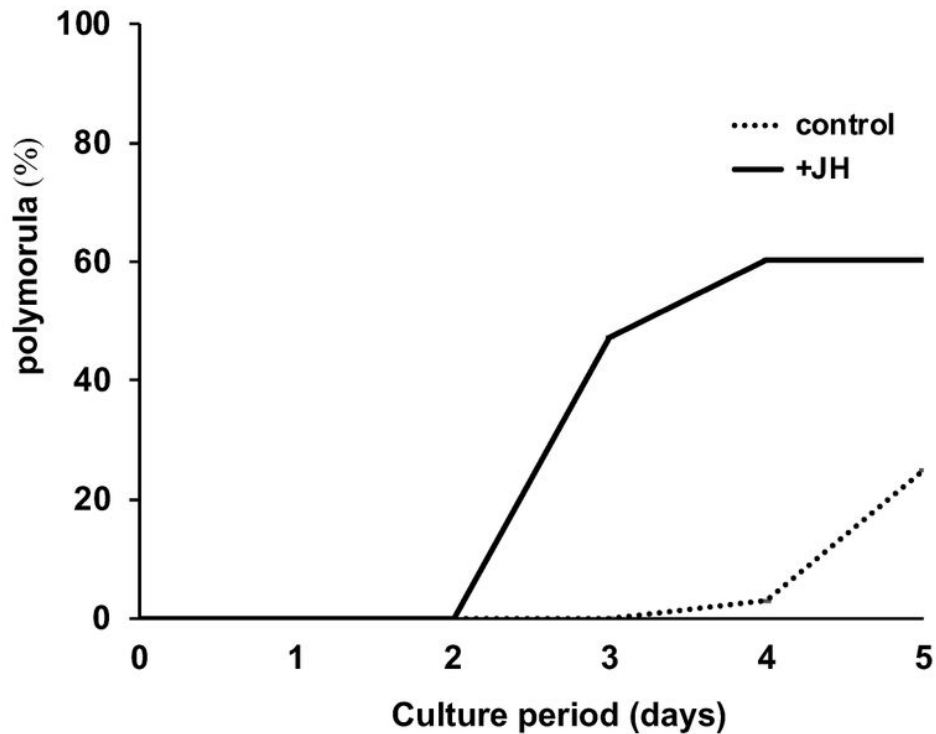


Figure 2

Polymorula was accelerated by the juvenile hormone (JH) treatment in the culture condition. The early embryo of the two-cell stage was cultured with or without JH. The number of polymorula was counted and plotted on the graph. Solid line, JH treatment; dashed line, treatment without JH; vertical axis, a rate of polymorula (%); horizontal axis, the culture period (day).

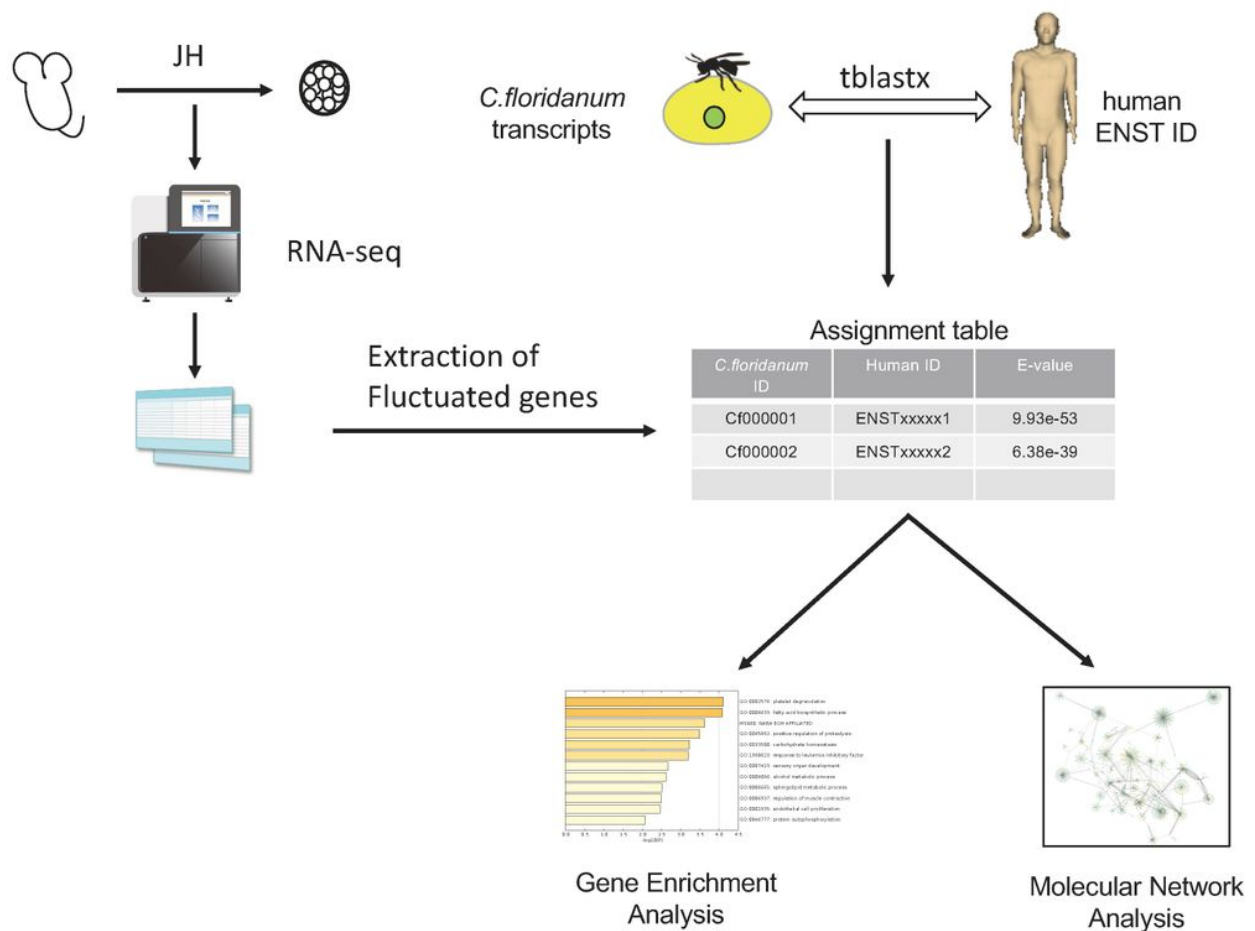


Figure 3

The strategy of annotation of *Copidosoma floridanum* transcript to human genes. We performed tblastx between *C. floridanum* transcripts and human transcripts on public databases to extract fluctuated genes in the juvenile hormone (JH) treatment using the RNA-Seq analysis. Then, we converted transcripts IDs from the *C. floridanum* RNA-Seq to human Ensembl IDs and constructed assignment table. Finally, we performed the gene enrichment analysis and molecular network analysis using the public database and determined molecular interaction in the polyembryogenesis. The experimental tools, human and machines drawings (<https://togotv.dbcls.jp/ja/pics.html>) are licensed under Creative Commons Attribution 4.0 International License (CC BY 4.0) (<http://creativecommons.org/licenses/by/4.0/deed.en>).

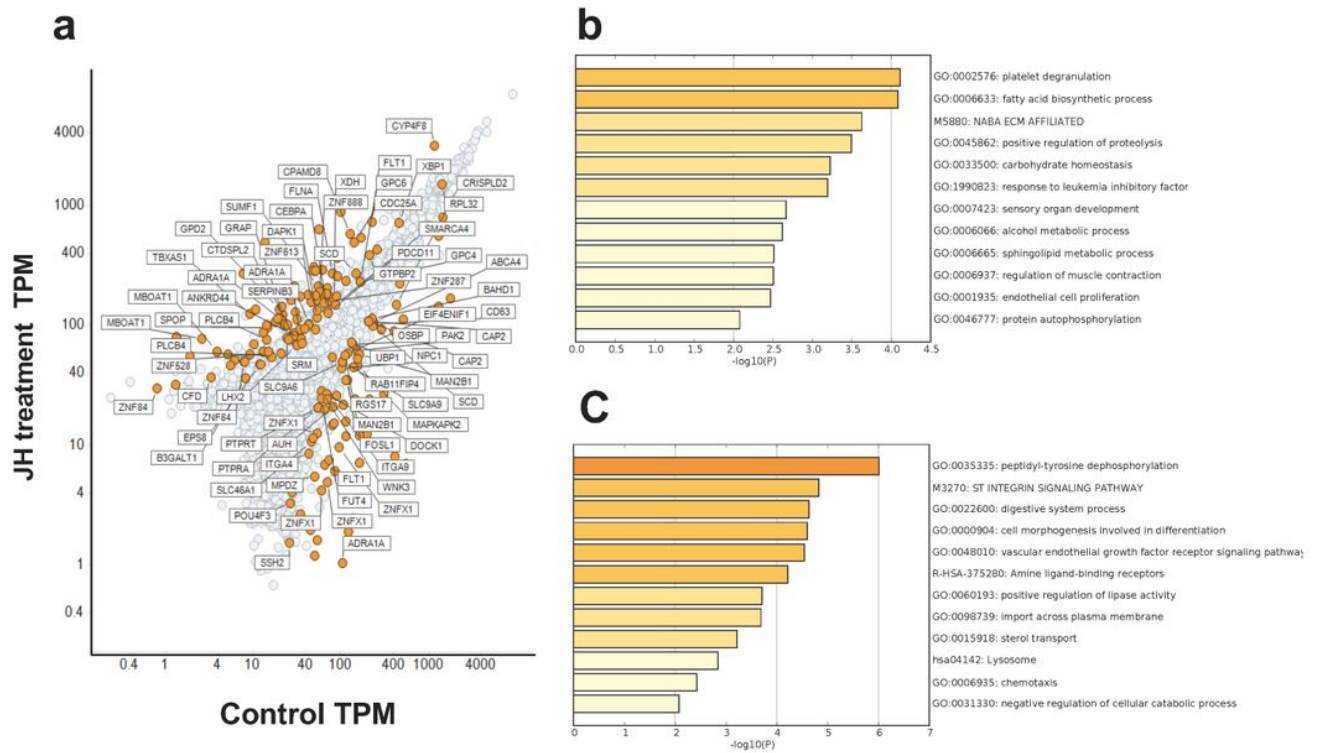


Figure 4

The extraction of fluctuated transcripts in the juvenile hormone (JH) treatment and gene enrichment analysis. Fluctuated transcripts were extracted and plotted on the graph. Orange dots, transcripts that fluctuated more than two times compared with the control in the JH treatment (a). The gene enrichment analysis of fluctuated transcripts in the morula using Metascape. A heatmap of enriched terms across the input transcripts lists; different colored bars, P values. (b) JH upregulated genes; (c) JH downregulated genes.

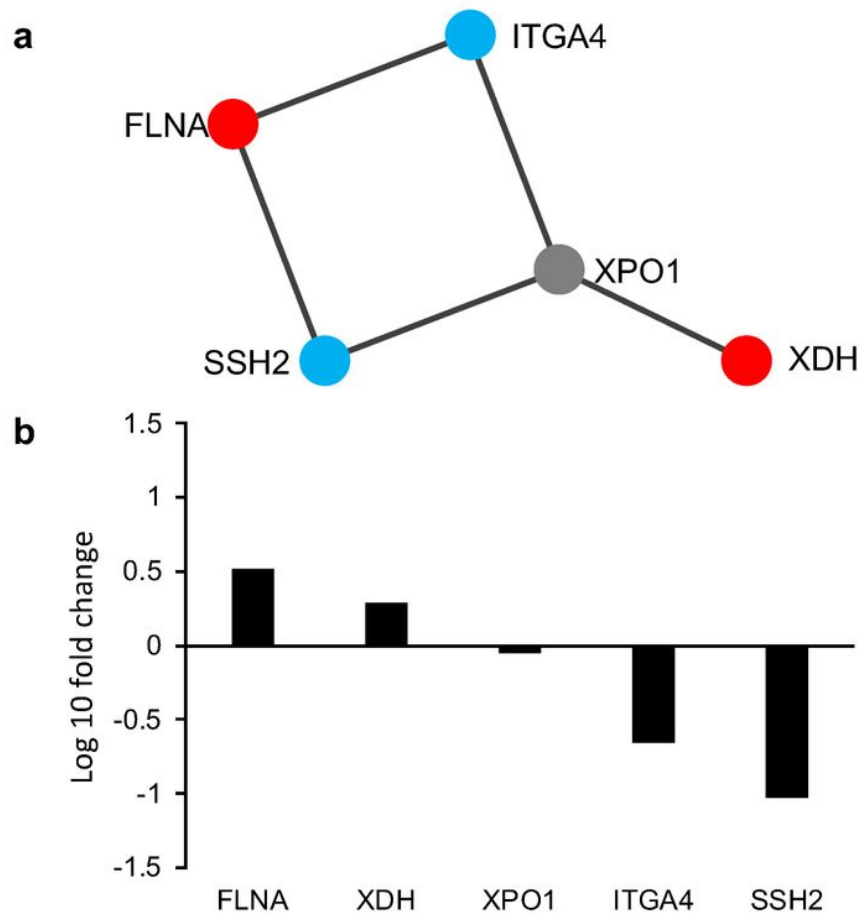


Figure 5

Screening of the molecular interaction using Cytoscape. The molecular interaction of (a) Cytoscape automatically generates the corresponding molecules as a node on a molecular Interaction in polyembryogenesis-related genes. A red colored node shows up-regulated genes, blue colored genes shows down-regulated genes, and a gray colored gene is not fluctuation gene. (b) Polyembryogenesis-related genes in juvenile hormone (JH) treatment of molura. The y-axis indicates the ratio of the average Transcripts Per Kilobase Million (TPM) values for molura between the control and JH treatment groups.

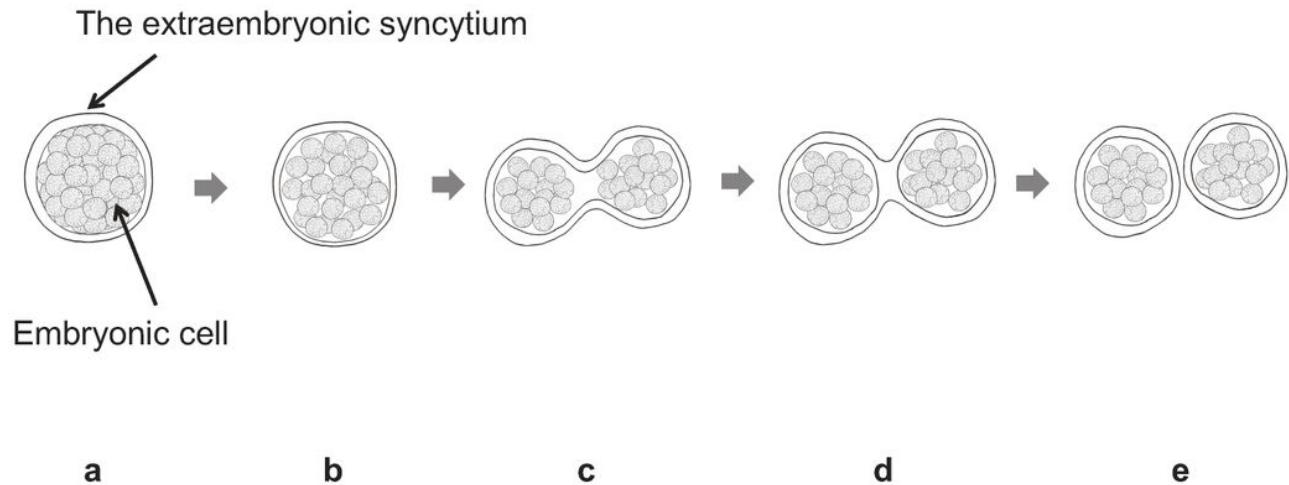


Figure 6

The model for the molecular mechanism of polyembryogenesis in *Copidosoma floridanum*. (a) The embryonic cell and the extraembryonic syncytium are attached in the molura. (b) The juvenile hormone (JH) loosens the cell attachment between the embryonic cells and the extraembryonic syncytium. (c) The extraembryonic syncytium invaginate into the molura. (d) After the inside of the extraembryonic syncytium has fused, (e) each cell is separated and polymorula are formed.

Supplementary Files

This is a list of supplementary files associated with this preprint. Click to download.

- [supplement1.docx](#)
- [supplement2.tiff](#)
- [supplement3.tiff](#)